Bone 187 (2024) 117200

Contents lists available at ScienceDirect

Bone

journal homepage: www.elsevier.com/locate/bone

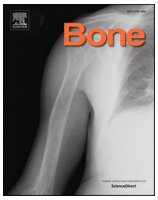

Full Length Article

Role of sclerostin deletion in bisphosphonate-induced osteonecrosis of the jaw

Fuminori Nakashima [a,1], Shinji Matsuda [a,*,1], Yurika Ninomiya [a], Tomoya Ueda [a], Keisuke Yasuda [a], Saki Hatano [a], Shogo Shimada [a], Daisuke Furutama [b], Takumi Memida [c], Mikihito Kajiya [d], Chisa Shukunami [e], Kazuhisa Ouhara [a], Noriyoshi Mizuno [a]

[a] Department of Periodontal Medicine, Graduate School of Biomedical and Health Sciences, Hiroshima University, Japan
[b] Department of Biological Endodontics, Graduate School of Biomedical and Health Sciences, Hiroshima University, Japan
[c] Department of Oral Science and Translation Research, College of Dental Medicine, Nova Southeastern University, United States of America
[d] Center of Oral Clinical Examination, Hiroshima University Hospital, Japan
[e] Department of Molecular Biology and Biochemistry, Graduate School of Biomedical and Health Sciences, Hiroshima University, Hiroshima, Japan

ARTICLE INFO

Keywords:
Medication-induced related osteonecrosis of the jaw
Sclerostin
Bone formation
Extraction socket healing

ABSTRACT

Purpose: Bone resorption inhibitors, such as bisphosphonates (BP) and denosumab, are frequently used for the management of osteoporosis. Although both drugs reduce the risk of osteoporotic fractures, they are associated with a serious side effect known as medication-related osteonecrosis of the jaw (MRONJ). Sclerostin antibodies (romosozumab) increase bone formation and decrease the risk of osteoporotic fractures: however, their anti-resorptive effect increases ONJ. Thus, this study aimed to elucidate the role of sclerostin deletion in the development of MRONJ.

Methods: Sclerostin knockout ($Sost^{\Delta 26/\Delta 26}$) mice were used to confirm the development of ONJ by performing tooth extractions. To confirm the role of sclerostin deficiency in a more ONJ-prone situation, we used the BP-induced ONJ model in combination with severe periodontitis to evaluate the development of ONJ and bone formation in wild-type (WT) and $Sost^{\Delta 26/\Delta 26}$ mice. Wound healing assay using gingival fibroblasts with or without sclerostin stimulation and tooth extraction socket healing were evaluated in the WT and $Sost^{\Delta 26/\Delta 26}$ mice.

Results: ONJ was not detected in the extraction socket of $Sost^{\Delta 26/\Delta 26}$ mice. Moreover, the incidence of ONJ was significantly lower in the $Sost^{\Delta 26/\Delta 26}$ mice treated with BP compared to that of the WT mice. Osteogenic proteins, osteocalcin, and runt-related transcription factor 2, were expressed in the bone surface in $Sost^{\Delta 26/\Delta 26}$ mice. Recombinant sclerostin inhibited gingival fibroblast migration. The wound healing rate of the extraction socket was faster in $Sost^{\Delta 26/\Delta 26}$ mice than in WT mice.

Conclusion: Sclerostin deficiency did not cause ONJ and reduced the risk of developing BP-induced ONJ. Enhanced bone formation and wound healing were observed in the tooth extraction socket. The use of romosozumab (anti-sclerostin antibody) has proven to be safe for surgical procedures of the jaw.

1. Introduction

Nitrogen-containing bisphosphonates (BP), such as zoledronic acid, alendronic acid, and pamidronate; and anti-receptor activator of nuclear factor kappa-B ligand antibodies, such as denosumab, can be used for the treatment and management of hypercalcemic bone metastases in patients with cancer [1,2] and prevention of fragility fractures in patients with osteoporosis [3]. Resorption inhibitors, including BP, are associated with a potentially serious adverse event, medication-related osteonecrosis of the jaw (MRONJ), which is defined as bone exposure in the maxillofacial region for >8 weeks in patients treated with resorption inhibitors without prior radiation therapy or metastatic jaw

Abbreviations: BP, bisphosphonates; μCT, micro computed tomography; HE, hematoxylin and eosin; MRONJ, medication-related osteonecrosis of the jaw; ONJ, osteonecrosis of the jaw; RUNX2, runt-related transcription factor 2; $Sost^{\Delta 26/\Delta 26}$, Sclerostin knockout; TBS, Tris-buffered saline.

* Corresponding author at: Department of Periodontal Medicine, Graduate School of Biomedical and Health Sciences, Hiroshima University, 1-2-3 Kasumi, Minami-ku, Hiroshima 734-8553, Japan.
E-mail address: matsudas@hiroshima-u.ac.jp (S. Matsuda).

[1] These two authors contributed equally to this work

https://doi.org/10.1016/j.bone.2024.117200
Received 17 May 2024; Received in revised form 4 July 2024; Accepted 9 July 2024
Available online 15 July 2024

disease as per the American Association of Oral and Maxillofacial Surgeons (AAOMS) [4].

Sclerostin, produced and secreted by mature osteocytes, blocks the activation of the Wnt/β-catenin osteogenic pathway in osteoblasts by reducing bone formation [5]. Physiologically, osteocytes decrease sclerostin release in response to mechanical stimuli acting on the bone, thus actively regulating bone mass in response to increased mechanical demands [6,7]. Loss of function mutations in human *SOST*, the gene encoding sclerostin, cause sclerosing ossification [8], which has been confirmed in multiple *Sost*-deficient mice [9–11]. The use of romosozumab, a neutralizing antibody that inhibits sclerostin, has been approved in several countries for the treatment of osteoporosis, which has a high risk of fractures. Romosozumab exerts a dual effect on bone by stimulating bone formation and inhibiting bone resorption [12–14]. Osteogenesis attributed to romosozumab results from the upregulation of Wnt signaling [15,16].

However, since romosozumab can potentially inhibit bone resorption, it can cause osteonecrosis of the jaw (ONJ). Romosozumab reduced the risk of osteoporotic fractures in a phase III osteoporosis trial; however, two cases of ONJ were reported in patients treated with romosozumab [12]. Furthermore, based on the US Food and Drug Administration Adverse Event Reporting System database, a real-world MRONJ data analysis revealed that ONJ was associated with romosozumab administration; nevertheless, its occurrence was much less frequent than that with BP [17]. In addition, although the direct effect of romosozumab is unknown, case reports have revealed severe ONJ in patients administered romosozumab [18]. In contrast, a previous experimentally validated study demonstrated that romosozumab did not induce ONJ in a periodontitis mouse model [19]. Thus, we investigated cases with a complete lack of sclerostin function to examine the role of sclerostin in MRONJ development using a mouse model lacking *Sost* ($Sost^{\Delta 26/\Delta 26}$ mouse model) – the gene encoding sclerostin [11]. Specifically, this study aimed to evaluate the effects of sclerostin on ONJ development and jawbone osteogenesis, and clarify the mechanism of action of MRONJ using the $Sost^{\Delta 26/\Delta 26}$ mouse model in combination with a model of ONJ development.

2. Materials and methods

2.1. Animal experiments

A minimal number of mice was used in each experiment. G*Power software was used to calculate the required sample size (significance level, 0.05, power of 0.8 or 0.9). Mice were kept in a vivarium at a room temperature of 22 ± 2 °C with a 12-h light/dark cycle (lights on/off at 8:00 am/8:00 pm) and were allowed unlimited access to food and water throughout the experimental period. All the animal experiments were conducted in accordance with the Guidelines for the Care and Use of Laboratory Animals established by the Japanese Pharmacological Society and Hiroshima University, and were reviewed and approved by the Hiroshima University Laboratory Animal Research Facility Committee (A19-83). We used $Sost^{\Delta 26/\Delta 26}$ mice lacking sclerostin due to a frameshift mutation introduced by Platinum TALENs [11]. Experiments were performed in wild-type (WT) and homozygous $Sost^{\Delta 26/\Delta 26}$ mice of the same litter (Supplemental Fig. 1). For genotyping, genomic DNA was extracted from the mouse tail, and polymerase chain reaction was performed using a specific primer set (Sost_GTF3:5′-CCCGTGCCTCATCTGCCTACTTG-3′; Sost_GTR2:5′-TCTTCATCCCGTACCTTTGGC-3′).

We extracted the maxillary first molar of the WT and $Sost^{\Delta 26/\Delta 26}$ mice to evaluate the onset of osteonecrosis following tooth extraction. After tooth extraction, histological evaluation, intraoral photography, and morphological examination of bone formation were performed for 1–3 weeks to assess the success or failure of extraction socket healing. ONJ models in association with BP were established based on previous studies [20–23]; to ensure more severe and consistent ONJ, a silk ligature-induced periodontitis combined extraction model was employed. The establishment of this model is shown in Fig. 2A. BP (disodium pamidronate; 1 mg/kg, Tokyo Chemical Industry, Japan) or vehicle was intraperitoneally administered once every 2 days for 2 weeks prior to ligating silk threads on the maxillary second molars of WT and $Sost^{\Delta 26/\Delta 26}$ mice with a modification of a previous report [24]. The teeth were extracted 1 week after ligation, and bone exposure in the oral cavity was assessed 1 week later; bone formation was evaluated using microcomputed tomography (μCT) and histologic analysis.

2.2. Histological evaluation

Mouse maxillary bones were demineralized with 10 % ethylenediaminetetraacetic acid for 1 week, dehydrated with ethanol and xylene, and embedded in paraffin; 8-μm thick sections were sequentially cut from the buccal palatal membrane, stained with hematoxylin-eosin (HE), and observed under a light microscope for histomorphometric analysis. For the histological evaluation of the extraction socket, sagittal sections were prepared, the root in the first or third molar was identified, and serial sections were created for evaluation. The middle of the extraction socket region was considered for analyzing bone formation upon HE staining; its area was 310 μm × 233 μm. One section per extraction socket was analyzed using ImageJ software. Jaw osteonecrosis was evaluated as per previous reports; briefly, the bonelike tissue apart from the alveolar bone, empty osteocyte lacunae, and surrounding multinuclear cells indicated the presence of necrotic bone in the extraction socket area. The distance between the two sections was 60 μm from the center of the extraction socket [25]. The osteonecrotic area in the alveolar bone of the extraction socket adjacent to the first molar was used to measure. The percentage of necrotic bone area per bone area from the alveolar bone crest to the root apex was measured. Necrotic bone was defined as an area with five or more contiguous osteocyte-free bone lumens and multinucleated giant cells on the bone surface as in previous reports [26–28].

2.3. Immunohistochemistry

Formalin-fixed, paraffin-embedded tissues were rehydrated by xylene infiltration and ethanol dilution. The tissue was activated at room temperature for 20 min in a wet box using Liberate Antibody Binding Solution (Polysciences, PA). The slides were then washed with tris-buffered saline (TBS) and inactivated with 3 % H_2O_2 for 10 min at room temperature to inactivate endogenous peroxidases. The slides were subsequently blocked to prevent nonspecific binding of antibodies using 5 % normal goat serum (Jackson ImmunoResearch Laboratories) for 60 min at room temperature. Primary antibodies, including mouse anti-SOST/Sclerostin antibody (R&D Systems, MN, AF1589), rabbit anti-osteocalcin (OCN) antibody (Proteintech, IL, 23418–1-AP), and rabbit anti-RUNX2 antibody (Abcam, UK, ab192256), were applied at 4 °C in a humidity chamber.

After washing with TBS, the slides were incubated with horseradish peroxidase-conjugated secondary antibodies (goat anti-rabbit IgG [H + L] antibody, Proteintech, SA00001-2; Goat anti-mouse IgG [H + L], Biotech, HAF109) for 30 min at room temperature. The tissues were washed with TBS, incubated with DAB (Liquid DAB+ Substrate/Chromogen System, Agilent, CA, Dako K3468), and washed with distilled water to end the reaction. The slides were counterstained with hematoxylin. As a positive control for RUNX2 and OCN, we identified that the cells lining the normal alveolar bone in the tooth extraction socket were positively expressed, while on the same section we confirmed that the expressions were not detected in gingival fibroblasts. Negative controls were obtained by omitting the primary antibodies. The positive control for sclerostin was osteocytes from the alveolar bone of wild-type mice. The first and third molars and furcation involvement of the alveolar bone of the second molar in the extraction socket were analyzed. The bone within the extraction socket of the proximal root of the second molar was measured. The length of the bone surface and the number of

immunostained cells were measured using ImageJ software. Six sections were examined from each group.

2.4. Microcomputed tomography (μCT) and bone loss analysis

Imaging using μCT was conducted at the Kureha Special Laboratory (Fukushima, Japan). The extracted maxilla was imaged using μCT (Scan Xmate-L090H, Comscantecno, Japan) at 76 kV, 105 μA, magnification of 18.5321×, resolution of 13.706 μm/pixel, and slice thickness of 13.706 μm. Multiple-slice imaging was performed on the first to third molars, and the images were captured in a tiff format in three directions. The CTAN (BRUKER, MA) analysis software was used to analyze the radiographic data. The bone volume/tissue volume ratio was measured to evaluate the amount of bone formation in the extraction socket. The region of interest was set within the extraction socket of the second molar, with the height at the cementoenamel junction of the first molar and width along the floor of the maxillary sinus. Bone tissue formation was calculated as a threshold over 33 tonal values in an 8 bit (256 tone) CT image, divided into two parts: bone tissue and soft tissue. To prevent differences among each sample according to the morphology of the alveolar bone, we evaluated the thickness of the 50 layers based on the area where the alveolar ridge of the bifurcation equivalent of the second molar was visible (13.706 μm/layer).

2.5. Wound healing in the extraction socket

To evaluate the wound healing process of gingival tissue following tooth extraction, gingival epithelium healing in the extraction socket in the WT and $Sost^{\Delta 26/\Delta 26}$ mice was assessed. The evaluation was performed according to the methodology reported in a previous paper [29]. Intraoral photographs were taken continuously for up to 6 days after tooth extraction. The percentage reduction in the extraction socket area of the gingiva was evaluated based on the size of the extraction socket at baseline (day 0 after tooth extraction).

2.6. Cell culture and wound healing assay

Gingival fibroblasts established from knockout mice were used, and a wound healing assay was performed according to previous methods [30]. After reaching confluence, the monolayers were washed twice with phosphate buffered saline, and the cells were scratched with a pipette tip and evaluated by counting the migrating cells in the scratched area 48 h after stimulation, or without stimulation using recombinant human sclerostin protein (100–49-1MG, Thermo Scientific, MA).

2.7. Statistical analysis

Statistical analyses were performed using JMP Pro, ver. 17. Differences between the means of three or more groups were analyzed using Tukey's multiple comparison test or Dunnett's test for normally distributed data, and Steel–Dwass's test for non-normally distributed data. Between-group comparisons of binary variables were performed using the $\chi 2$ or Fisher's exact tests. Odds ratios and 95 % confidence intervals were computed using multivariable logistic regression analysis with Firth's correction to evaluate the influence of gene alteration on ONJ development adjusted with or without BP application. The extent of the extraction socket based on the time and genetic variability in cell migration ability was evaluated using Tukey's multiple comparison test for determining the extent of the reduced area of the extraction socket in the WT and $Sost^{\Delta 26/\Delta 26}$ mice for each day, following evaluation by two-way analysis of variance after an interaction between time and genetic background was confirmed. An alpha level of 0.05 was used throughout the study.

3. Results

We used *Sost*-deletion mice, which have a 26-base-pair (bp) deletion causing a frameshift that leads to a premature stop codon immediately downstream [11]. The wild-type allele in $Sost^{+/+}$ mice corresponds to a 211-bp band and the mutant allele in $Sost^{\Delta 26/\Delta 26}$ mice lacking sclerostin to a 185-bp band (Supplemental Fig. 1A). Loss of sclerotin protein expression in the femur of $Sost^{\Delta 26/\Delta 26}$ mice was confirmed by western blotting (Supplemental Fig. 1B). We subsequently evaluated sclerostin expression in the alveolar bone and periodontal tissue of the WT and $Sost^{\Delta 26/\Delta 26}$ mice (Fig. 1A). Sclerostin expression was not limited to osteocytes, and was also observed in the periodontal ligament and gingival connective tissue in WT mice; however, sclerostin expression was not observed at any site in $Sost^{\Delta 26/\Delta 26}$ mice. Bone exposure and formation in the extraction socket were evaluated to confirm the development of extraction-induced ONJ. Bone exposure of the extraction socket was not observed in either WT or $Sost^{\Delta 26/\Delta 26}$ mice (Fig. 1B. $n = 8$). Histological evaluation of the extraction socket at 1 week revealed bone formation in $Sost^{\Delta 26/\Delta 26}$ mice (Fig. 1C); moreover, at 3 weeks, healing of the extraction socket was comparable to that in WT and $Sost^{\Delta 26/\Delta 26}$ mice (Supplemental Fig. 2).

Since we observed bone formation earlier in the extraction socket of $Sost^{\Delta 26/\Delta 26}$ mice, we evaluated the effect of sclerostin deletion on the onset of BP-induced ONJ. To increase the risk of developing BP-induced ONJ, we used a model in which BP was combined with periodontitis and silk thread ligation. The results revealed that although bone exposure in the extraction socket was observed in WT mice treated with BP, no bone exposure was observed in $Sost^{\Delta 26/\Delta 26}$ mice in either the BP-untreated or BP-treated groups. In addition, necrotic bone tissue was identified at seven sites in WT mice treated with BP; however, osteonecrosis-like tissue was identified at only one site in $Sost^{\Delta 26/\Delta 26}$ mice treated with BP (Fig. 2B). Quantitative evaluation of socket healing and ONJ between the groups confirmed significant differences (Table 1). Additionally, a strong influence of *Sost* deletion on ONJ development was observed (Table 1). In addition, the osteonecrotic area in the alveolar bone was evaluated (Supplementary Fig. 3). The osteonecrotic bone area was significantly reduced in vehicle-treated $Sost^{\Delta 26/\Delta 26}$ mice compared to BP-treated WT mice. The area in BP-treated $Sost^{\Delta 26/\Delta 26}$ mice was reduced compared to WT mice, but not significantly. Thereafter, μCT was used to quantitatively evaluate the amount of bone formation in the extraction socket. Compared to WT mice, higher bone volume in the extraction socket was observed in the $Sost^{\Delta 26/\Delta 26}$ mouse group, both with and without BP administration (Fig. 2C).

Osteogenesis-related protein (OCN and runt-related transcription factor 2 [RUNX2]) expression was evaluated in the extraction socket of WT and $Sost^{\Delta 26/\Delta 26}$ mice. OCN and RUNX2 positive cells were significantly increased at osteogenic sites in the extraction socket of $Sost^{\Delta 26/\Delta 26}$ mice, while their expressions (OCN and RUNX2) were significantly lower in the WT mice (Fig. 3A, B).

Finally, as delayed epithelial coverage of the extraction socket is associated with MRONJ development, we tested whether sclerostin is associated with gingival wound healing after tooth extraction. Recombinant sclerostin significantly inhibited gingival fibroblast migration (Fig. 4A). We also evaluated the differences in gingival tissue healing in the extraction socket of the wound healing model. Wound healing of the extraction socket progressed earlier in $Sost^{\Delta 26/\Delta 26}$ mice compared with that in WT mice, with significant differences from day 3; moreover, healing was nearly complete by day 6. The results of the two-way analysis of variance for differences in the time factor and genetic background of wound healing are shown in Table 2.

4. Discussion

In this study, we demonstrated for the first time the inhibitory effect of sclerostin deficiency on ONJ in combination with BP and periodontitis. In addition, sclerostin deletion promoted bone formation and the

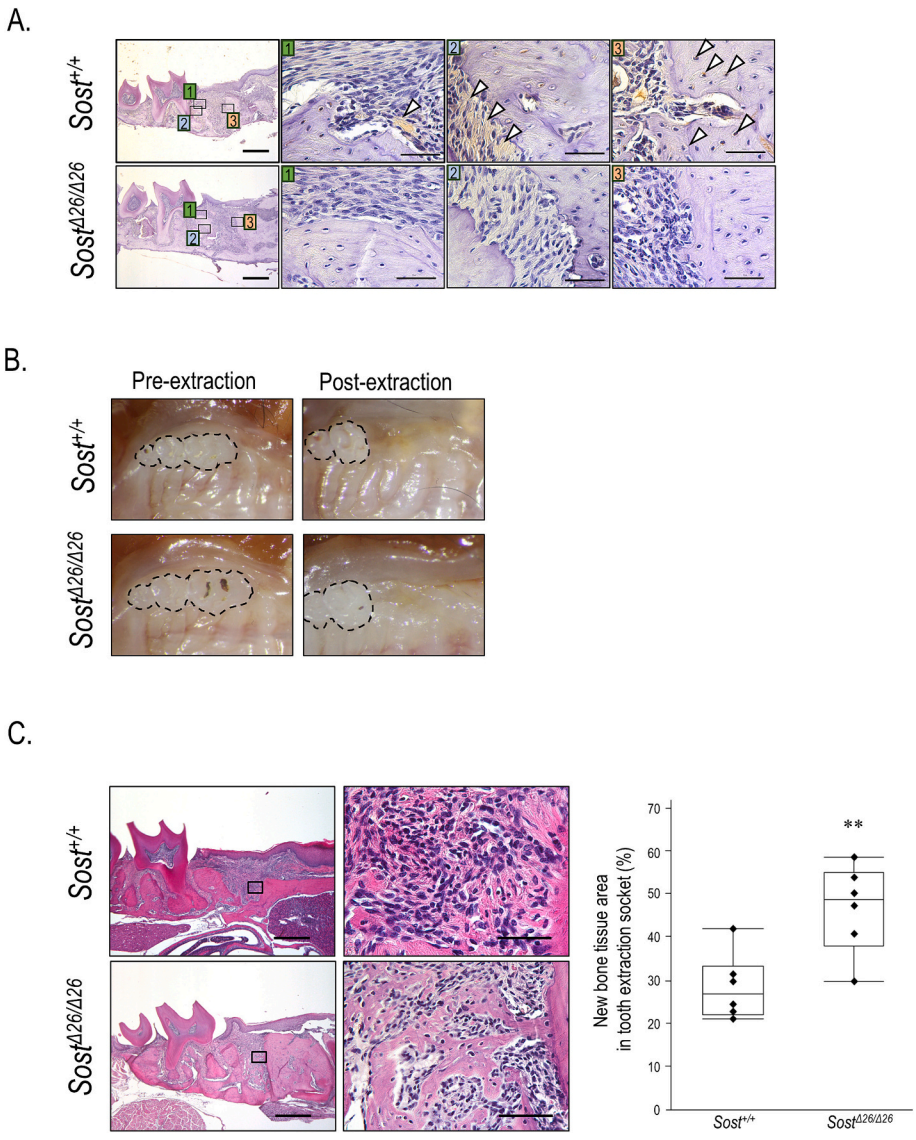

Fig. 1. Role of sclerostin deletion in the development of osteonecrosis of the jaw. A. Immunostaining of sclerostin in the gingival connective tissue (1), periodontal ligament (2), and alveolar bone (3). White arrowhead shows sclerostin expression. Bar = 50 μm B. The intraoral photo of the pre- and 3 weeks post-extraction of the first molar in the maxillae. C. Hematoxylin staining of the extraction socket 1 week after extraction. Lower magnification in the upper image and higher magnification in the lower image. Bar = 500 μm (lower magnification). Bar =50 μm (higher magnification). The graph shows the bone formation area compared between the $Sost^{\Delta 26/\Delta 26}$ and wild-type mice. $n = 6$. Median (interquartile range, IQR). $^{**}p < 0.01$.

expression of bone-related proteins in the extraction socket. Furthermore, epithelial wound healing was accelerated in *Sost* knockout mice compared with that in WT mice.

The risk of ONJ development has been reported following the use of romosozumab – a neutralizing antibody against sclerostin. However, to date, reports of romosozumab-induced ONJ are less frequent than those of other ONJ-inducing agents and are insufficiently substantiated to indicate a clear risk [17]. Moreover, romosozumab did not induce ONJ in a previous study on silk ligation-induced periodontitis rat model [19]. The present study more strongly mimics the administration of romosozumab; moreover, $Sost^{\Delta 26/\Delta 26}$ mice were used to evaluate the effect of first molar extraction on ONJ development and bone formation. First, we evaluated sclerostin expression in the jawbones. Consistent with previous reports [31], sclerostin expression was observed in the alveolar bone osteocytes, periodontal ligament, and gingival connective tissue, but not in the *Sost* knockout mice. Bone exposure in the oral cavity after tooth extraction was not observed in either WT or $Sost^{\Delta 26/\Delta 26}$ mice. Furthermore, bone morphology evaluation of the extraction socket revealed accelerated bone formation in the knockout mice 1 week after tooth extraction. These results suggest that the lack of sclerostin does not cause ONJ during tooth extraction, but rather promotes bone formation in the extraction socket.

The MRONJ model was used to evaluate the effects of sclerostin on ONJ development. To replicate a more severe situation, we used a model in which silk-ligated periodontitis in combination with BP increased the frequency of onset and worsened the severity of the disease compared with the use of BP alone [22,23]. The results revealed that the number of intraoral bone exposures was significantly suppressed in the $Sost^{\Delta 26/\Delta 26}$ mice with or without BP. Furthermore, the presence of necrotic jaw bone was also significantly reduced in $Sost^{\Delta 26/\Delta 26}$ mice compared to WT male and female mice (Supplemental Fig. 5). This finding suggests that sclerostin deletion has a low risk of direct involvement in the development of BP-induced ONJ. Since sclerostin deletion causes increased bone density [11], we evaluated whether bone formation was also enhanced by BP treatment using CT imaging. The results demonstrated enhanced bone formation in the extraction socket of $Sost^{\Delta 26/\Delta 26}$ mice compared to

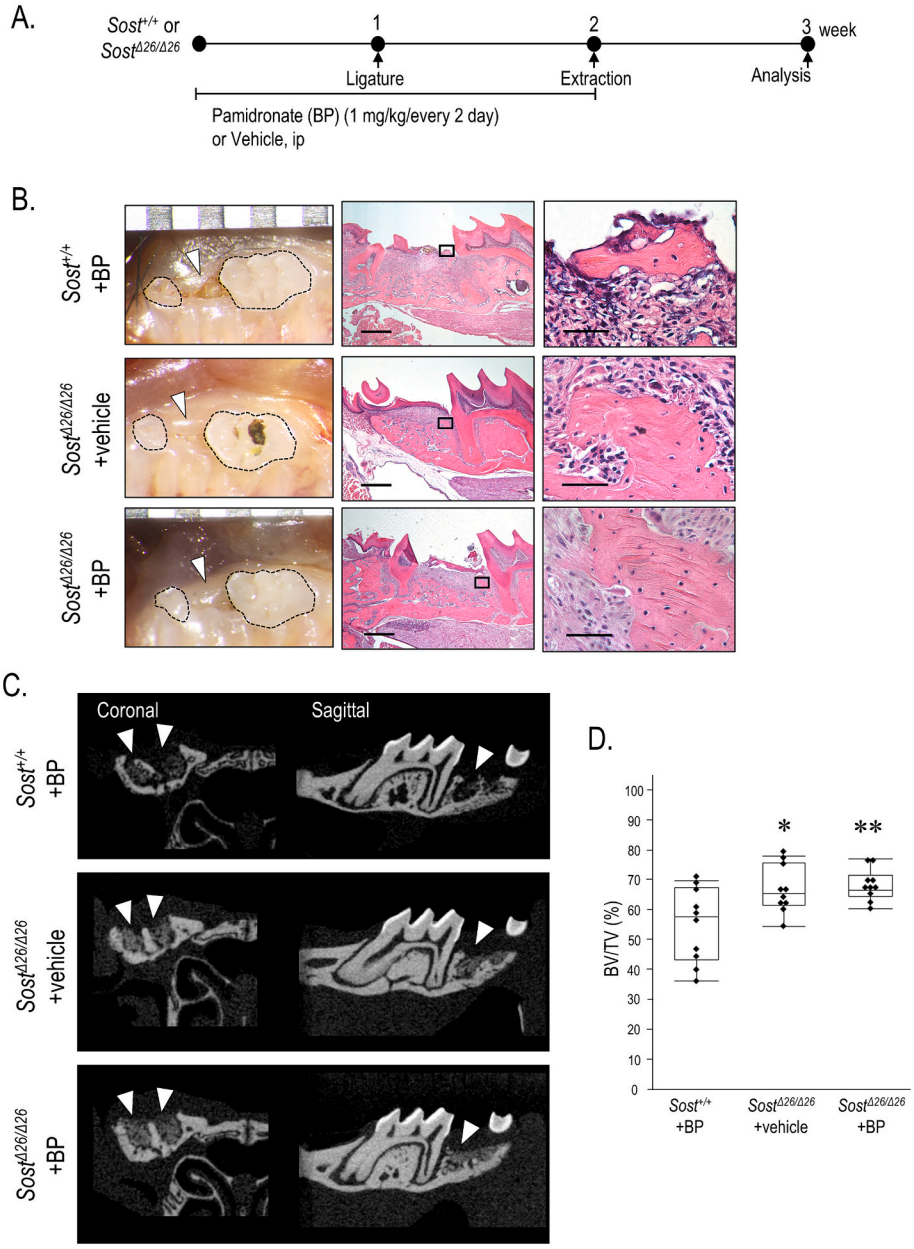

Fig. 2. Role of sclerostin deletion in bisphosphonate (BP) induced osteonecrosis of the jaw (ONJ) development. A. Schedule of the experiment. B. Oral photograph in the left images. Hematoxylin and eosin staining in lower magnification; middle images. Higher magnification; right images. Bar = 500 μm (lower magnification). Bar =50 μm (higher magnification). C. Micro-computed tomography image in the maxillae after tooth extraction. White arrowheads show extraction socket. D. Quantitative analysis of bone volume (BV)/tissue volume (TV) in the tooth extraction socket (%). TV is defined as original tooth extraction socket. BV is forming bone in the extraction socket. $n = 10$. Median (IQR). *$p < 0.05$, **$p < 0.01$.

that of WT mice. Bone formation in the extraction socket of a mouse model of MRONJ following tooth extraction was delayed by BP administration [32], and local administration of bone morphogenetic protein 2, which promotes bone formation, reportedly prevents ONJ development [33]. The suppression of BP-induced ONJ by *Sost*$^{\Delta 26/\Delta 26}$ mice may be attributed to the promotion of bone formation, which is delayed by BP administration. Therefore, we evaluated the expression of OCN and RUNX2, markers of osteoblast differentiation, in the extraction socket to indicate bone formation. The association between MRONJ and osteogenic proteins has been demonstrated previously, with low serum OCN levels associated with slower healing of jaw osteonecrosis rather than high OCN levels [34]. Furthermore, Wnt signaling—a target of sclerostin—is strongly associated with OCN and RUNX2 expression during osteoblast differentiation, which promotes bone formation [35]. The results of this study revealed that *Sost*$^{\Delta 26/\Delta 26}$ mice were more sensitive to osteoblast differentiation than WT mice; moreover, OCN and RUNX2 expression was strongly upregulated in the extraction socket of *Sost*$^{\Delta 26/\Delta 26}$ mice compared to that in WT mice. The expression of these two genes was also increased in the BP-treated group in the *Sost*$^{\Delta 26/\Delta 26}$ mice, indicating their potential role in the prevention and treatment of BP-induced ONJ development.

Next, we focused on the effect of sclerostin on wound healing of the gingival epithelium in the extraction socket based on several reports of delayed or impaired wound healing of the gingival epithelium, presumably contributing to the development of ONJ [36,37]. Gingival wound healing promotion reportedly prevents the development of MRONJ [38]. In this study, we evaluated the effect of recombinant sclerostin protein stimulation on the migration of gingival fibroblasts

Table 1
Association between *SOST* deletion and BP-induced ONJ development.

	$Sost^{+/+}$ + BP	$Sost^{\Delta 26/\Delta 26}$ + vehicle	$Sost^{\Delta 26/\Delta 26}$ + BP	Total	p
Socket healing delay	4	0	0	4	<0.05
Socket healing	6	10	10	26	
Total	10	10	10	30	
Necrotic bone	7	0	1	8	<0.01
No necrotic bone	13	20	19	52	
Total	20	20	20	60	

	Reference	OR	95 % CI	p
Gene alternation	WT	2.69	1.15, 8.62	0.01

BP, bisphosphonate; ONJ, osteonecrosis of the jaw; OR, Odds ratio; CI, confidence interval.
Fisher's exact test was conducted to compare the incidence rate of socket healing success/fail or exert of necrotic bone in the socket in WT or $Sost^{\Delta 26/\Delta 26}$ with and without BP. Firth's bias correction was used to accommodate the low frequency of outcomes. Multiple logistic regression was used to detect the effect of gene alteration on the observation of necrotic bone adjusted for BP treatment.

isolated from $Sost^{\Delta 26/\Delta 26}$ mice. Our results revealed that sclerostin administration inhibits cell migration. In addition, gingival wound healing was enhanced in the tooth extraction socket of $Sost^{\Delta 26/\Delta 26}$ mice compared to that of WT mice. Consistent with our data, studies have demonstrated inhibition of oral squamous carcinoma cell migration by sclerostin [39] and promotion of osteosarcoma cell migration [40] and uveal melanoma [41] by sclerostin deletion. Since sclerostin suppresses Wnt signaling, sclerostin deletion is expected to activate Wnt signaling and promote cell migration. The relationship among sclerostin deletion, gingival wound healing, and MRONJ should be further elucidated to aid the development of novel therapies for MRONJ.

This study has several limitations. First, the MRONJ model used had an ONJ onset when pamidronate was used and the duration of administration was 2 weeks. The effect of sclerostin deficiency on ONJ would be more evident if a more severe ONJ model (e.g., by using zoledronate for 4–6 weeks and dexamethasone, as reported in previous reports [26]) were used. Second, in the present study, osteonecrosis of the jaw was assessed by bone exposure of the extraction socket and separation of necrotic bone from the original alveolar bone, and the $Sost^{\Delta 26/\Delta 26}$ mice showed significantly less incidence of BP-induced osteonecrosis of the jaw compared to WT. However, when the bone morphology of the alveolar bone was evaluated, although there was a tendency for the bone area to decrease in $Sost^{\Delta 26/\Delta 26}$ mice treated with BP compared with WT, no significant difference was observed (Supplementary Fig. 3). The use of a severe model may allow a more accurate evaluation of the effects on bone tissue. Finally, tissue sections were prepared at 8 μm thickness for histological analysis. In this study, thicker sections were prepared to accurately evaluate empty bone lacunae. Thinner sections are more suitable for immunostaining to avoid tissue overlap.

5. Conclusion

Our study demonstrated for the first time that BP-induced ONJ is suppressed in mice lacking sclerostin, which in turn promotes accelerated bone formation and epithelial wound healing in the tooth extraction socket. The use of romosozumab (anti-sclerostin antibody) has proven to be safe for surgical procedures of the jaw. The underlying association between sclerostin and MRONJ should be further elucidated to develop novel therapies for MRONJ.

Supplementary data to this article can be found online at https://doi.org/10.1016/j.bone.2024.117200.

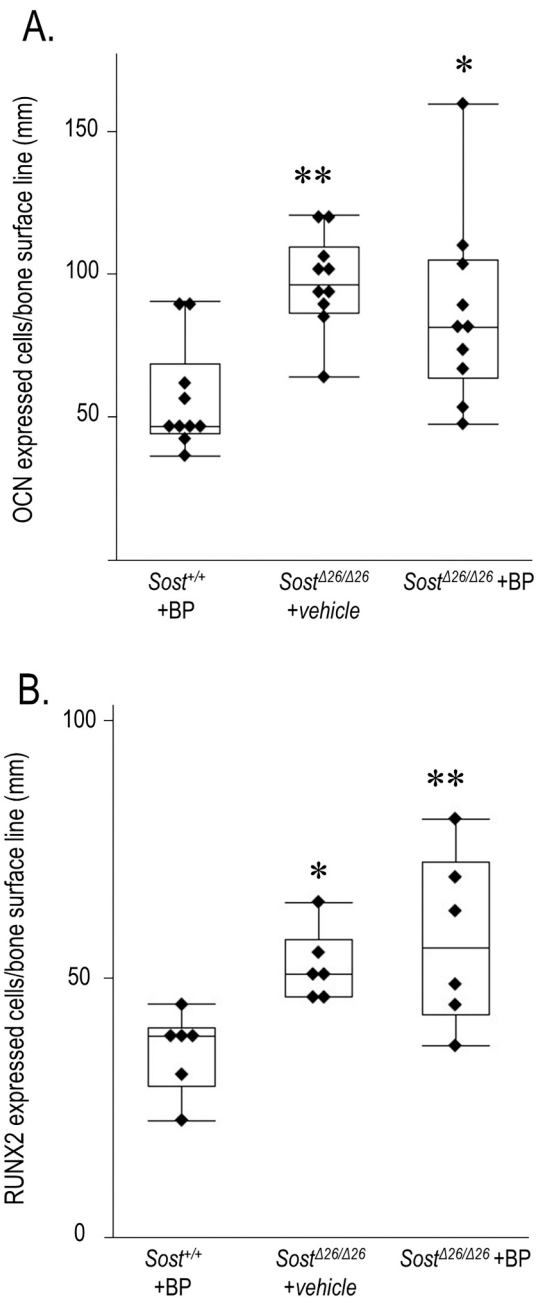

Fig. 3. The expression of bone-related protein in the tooth extraction socket. A. osteocalcin (OCN) expressed cells on the bone surface line in the extraction socket were counted. $n = 8$. Median (interquartile range, IQR). $^{*}p < 0.05$, $^{**}p < 0.01$. B. The number of runt-related transcription factor 2 (RUNX2) expressed cells on the bone surface line in the extraction socket. n = 6. Median (IQR). $^{*}p < 0.05$, $^{**}p < 0.01$.

CRediT authorship contribution statement

Fuminori Nakashima: Investigation, Funding acquisition. **Shinji Matsuda:** Writing – original draft, Methodology, Conceptualization. **Yurika Ninomiya:** Investigation. **Tomoya Ueda:** Investigation. **Keisuke Yasuda:** Investigation. **Saki Hatano:** Funding acquisition. **Shogo Shimada:** Investigation. **Daisuke Furutama:** Investigation. **Takumi Memida:** Data curation. **Mikihito Kajiya:** Supervision. **Chisa Shukunami:** Supervision. **Kazuhisa Ouhara:** Supervision. **Noriyoshi Mizuno:** Writing – review & editing, Supervision.

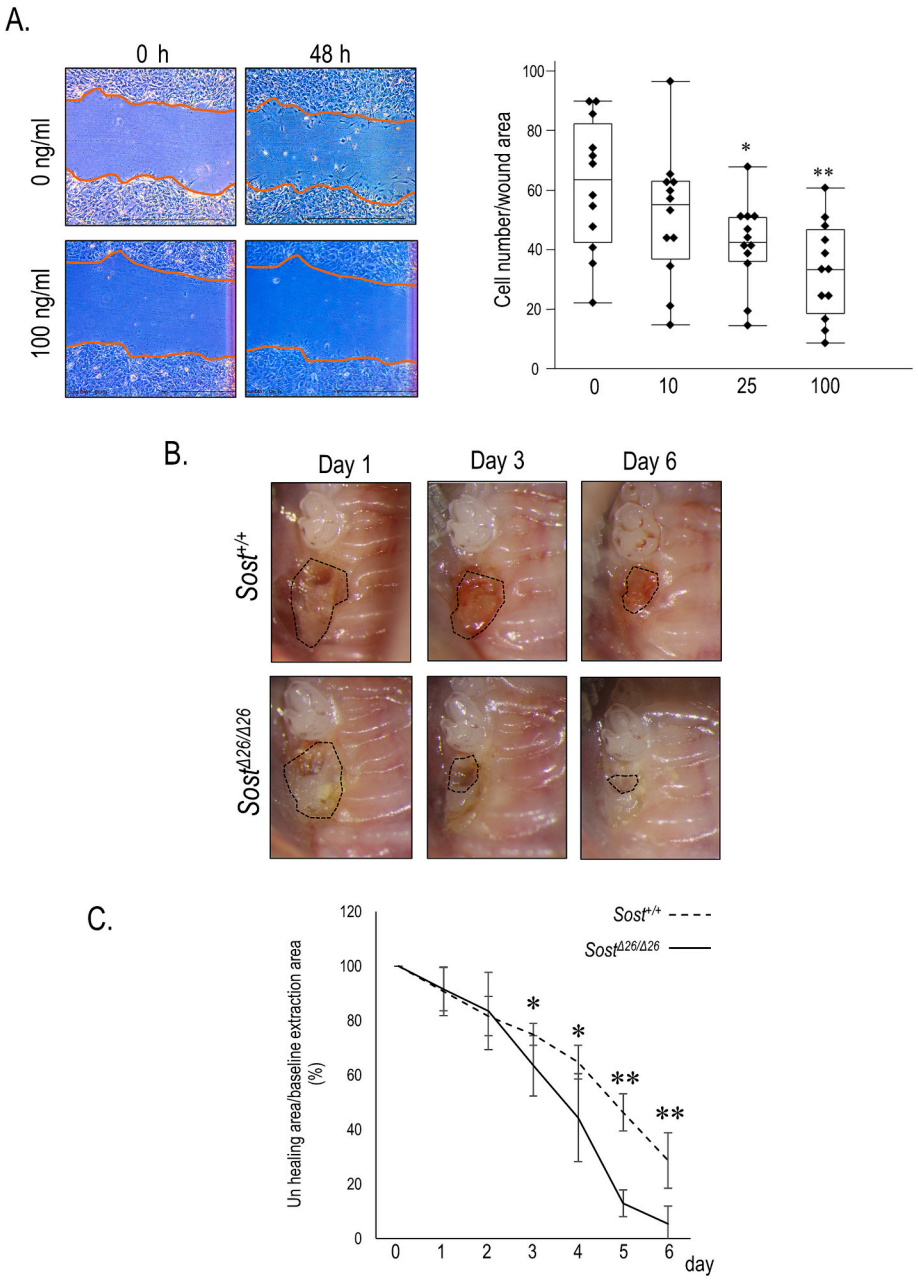

Fig. 4. Role of sclerostin on wound healing of gingival fibroblasts and gingiva in the tooth extraction socket. A. Wound healing assay. Migrated mouse gingival fibroblasts were evaluated by counting cells in the scratched area 48 h after stimulation or non-stimulation with recombinant human sclerostin protein. $n = 12$. Median (interquartile range, IQR). $^{*}p < 0.05$, $^{**}p < 0.01$. B. Comparison of the socket healing area between SOST knock-out (KO) and WT mice. C. Socket healing area in the SOST KO and WT mice. Multiple comparison test for determining the extent of the reduced area of the extraction socket in the WT and $Sost^{\Delta 26/\Delta 26}$ mice for each day, after evaluation by two-way analysis of variance. n = 6. Mean (standard deviation, SD). $^{*}p < 0.05$, $^{**}p < 0.01$.

Table 2
Two-way analysis of variance (ANOVA) was used for post-hoc Tukey's test to evaluate the factors associated with wound healing of the extraction socket.

	F	df	p
Time	188.53	6, 60	<0.0001
Group	21.3	1, 10	0.001
Time * group	9.2552	6, 60	<0.0001

Time * group indicates the interaction effect of time (day) and group (WT or $Sost^{\Delta 26/\Delta 26}$).
F: F value. *df*: degree of freedom.

Declaration of competing interest

There are no conflicts of interest to declare.

Data availability

The authors do not have permission to share data.

Acknowledgements

None.

Funding statement

This study was supported by JSPS KAKENHI (Grant number, 23K15973) and JST SPRING (Grant number, JPMJSP2132).

References

[1] I. Duran, M.G. Fink, A. Bahl, H. Hoefeler, A. Mahmood, D. Lüftner, H. Ghazal, R. Wei, K.C. Chung, G. Hechmati, J. Green, C. Atchison, Health resource utilisation associated with skeletal-related events in patients with bone metastases secondary to solid tumours: regional comparisons in an observational study, Eur J Cancer Care (Engl) 26 (6) (2017).

[2] C. Van Poznak, M.R. Somerfield, W.E. Barlow, J.S. Biermann, L.D. Bosserman, M. J. Clemons, S.K. Dhesy-Thind, M.S. Dillmon, A. Eisen, E.S. Frank, R. Jagsi, R. Jimenez, R.L. Theriault, T.A. Vandenberg, G.C. Yee, B. Moy, Role of bone-modifying agents in metastatic breast cancer: an American Society of Clinical Oncology-Cancer Care Ontario focused guideline update, J. Clin. Oncol. 35 (35) (2017) 3978–3986.

[3] E.W. Yu, E. Tsourdi, B.L. Clarke, D.C. Bauer, M.T. Drake, Osteoporosis management in the era of COVID-19, J. Bone Miner. Res. 35 (6) (2020) 1009–1013.

[4] S.L. Ruggiero, T.B. Dodson, T. Aghaloo, E.R. Carlson, B.B. Ward, D. Kademani, American association of oral and maxillofacial surgeons' position paper on medication-related osteonecrosis of the jaws-2022 update, J. Oral Maxillofac. Surg. 80 (5) (2022) 920–943.

[5] E.S. Vasiliadis, D.S. Evangelopoulos, A. Kaspiris, I.S. Benetos, C. Vlachos, S. G. Pneumaticos, The role of sclerostin in bone diseases, J. Clin. Med. 11 (3) (2022).

[6] X. Tu, J. Delgado-Calle, K.W. Condon, M. Maycas, H. Zhang, N. Carlesso, M. M. Taketo, D.B. Burr, L.I. Plotkin, T. Bellido, Osteocytes mediate the anabolic actions of canonical Wnt/β-catenin signaling in bone, Proc. Natl. Acad. Sci. USA 112 (5) (2015) E478–E486.

[7] G.L. Galea, L.E. Lanyon, J.S. Price, Sclerostin's role in bone's adaptive response to mechanical loading, Bone 96 (2017) 38–44.

[8] W. Balemans, M. Ebeling, N. Patel, E. Van Hul, P. Olson, M. Dioszegi, C. Lacza, W. Wuyts, J. Van Den Ende, P. Willems, A.F. Paes-Alves, S. Hill, M. Bueno, F. J. Ramos, P. Tacconi, F.G. Dikkers, C. Stratakis, K. Lindpaintner, B. Vickery, D. Foernzler, W. Van Hul, Increased bone density in sclerosteosis is due to the deficiency of a novel secreted protein (SOST), Hum. Mol. Genet. 10 (5) (2001) 537–543.

[9] X. Li, M.S. Ominsky, Q.T. Niu, N. Sun, B. Daugherty, D. D'Agostin, C. Kurahara, Y. Gao, J. Cao, J. Gong, F. Asuncion, M. Barrero, K. Warmington, D. Dwyer, M. Stolina, S. Morony, I. Sarosi, P.J. Kostenuik, D.L. Lacey, W.S. Simonet, H.Z. Ke, C. Paszty, Targeted deletion of the sclerostin gene in mice results in increased bone formation and bone strength, J. Bone Miner. Res. 23 (6) (2008) 860–869.

[10] N. Hassler, A. Roschger, S. Gamsjaeger, I. Kramer, S. Lueger, A. van Lierop, P. Roschger, K. Klaushofer, E.P. Paschalis, M. Kneissel, S. Papapoulos, Sclerostin deficiency is linked to altered bone composition, J. Bone Miner. Res. 29 (10) (2014) 2144–2151.

[11] S. Yambe, Y. Yoshimoto, K. Ikeda, K. Maki, A. Takimoto, A. Tokuyama, S. Higuchi, X. Yu, K. Uchibe, S. Miura, H. Watanabe, T. Sakuma, T. Yamamoto, K. Tanimoto, G. Kondoh, M. Kasahara, T. Mizoguchi, D. Docheva, T. Adachi, C. Shukunami, Sclerostin modulates mineralization degree and stiffness profile in the fibrocartilaginous enthesis for mechanical tissue integrity, Frontiers, Frontiers in Cell and Developmental Biology 12 (2024) 1360041.

[12] F. Cosman, D.B. Crittenden, J.D. Adachi, N. Binkley, E. Czerwinski, S. Ferrari, L. C. Hofbauer, E. Lau, E.M. Lewiecki, A. Miyauchi, C.A. Zerbini, C.E. Milmont, L. Chen, J. Maddox, P.D. Meisner, C. Libanati, A. Grauer, Romosozumab treatment in postmenopausal women with osteoporosis, N. Engl. J. Med. 375 (16) (2016) 1532–1543.

[13] P. Chavassieux, R. Chapurlat, N. Portero-Muzy, J.P. Roux, P. Garcia, J.P. Brown, C. Libanati, R.W. Boyce, A. Wang, A. Grauer, Bone-forming and antiresorptive effects of romosozumab in postmenopausal women with osteoporosis: bone histomorphometry and microcomputed tomography analysis after 2 and 12 months of treatment, J. Bone Miner. Res. 34 (9) (2019) 1597–1608.

[14] E.F. Eriksen, R. Chapurlat, R.W. Boyce, Y. Shi, J.P. Brown, S. Horlait, D. Betah, C. Libanati, P. Chavassieux, Modeling-based bone formation after 2 months of romosozumab treatment: results from the FRAME clinical trial, J. Bone Miner. Res. 37 (1) (2022) 36–40.

[15] S. Taylor, R. Hu, E. Pacheco, K. Locher, I. Pyrah, M.S. Ominsky, R.W. Boyce, Differential time-dependent transcriptional changes in the osteoblast lineage in cortical bone associated with sclerostin antibody treatment in ovariectomized rats, Bone Rep 8 (2018) 95–103.

[16] G. Holdsworth, K. Greenslade, J. Jose, Z. Stencel, H. Kirby, A. Moore, H.Z. Ke, M. K. Robinson, Dampening of the bone formation response following repeat dosing with sclerostin antibody in mice is associated with up-regulation of Wnt antagonists, Bone 107 (2018) 93–103.

[17] J. Peng, H. Wang, Z. Liu, Z.L. Xu, M.X. Wang, Q.M. Chen, M.L. Wu, X.L. Ren, Q. H. Liang, F.P. Liu, B. Ban, Real-world study of antiresorptive-related osteonecrosis of jaw based on the US food and drug administration adverse event reporting system database, Front. Pharmacol. 13 (2022) 1017391.

[18] B. Palla, J. Anderson, M. Miloro, S. Moles, N. Callahan, Romosozumab-associated medication-related osteonecrosis of the jaw, in: Oral and Maxillofacial Surgery Cases, Elsevier, 2023.

[19] D. Hadaya, I. Gkouveris, A. Soundia, O. Bezouglaia, R.W. Boyce, M. Stolina, D. Dwyer, S.M. Dry, F.Q. Pirih, T.L. Aghaloo, S. Tetradis, Clinically relevant doses of sclerostin antibody do not induce osteonecrosis of the jaw (ONJ) in rats with experimental periodontitis, J. Bone Miner. Res. 34 (1) (2019) 171–181.

[20] E. Ervolino, M.B. Olivo, L.F. Toro, J.O.A. Freire, V.F. Ganzaroli, I.Z. Guiati, M.A. A. Nuernberg, J.P.S. Franciscon, L.T. Ângelo Cintra, V.G. Garcia, M. Wainwright, L. H. Theodoro, Effectiveness of antimicrobial photodynamic therapy mediated by butyl toluidine blue in preventing medication-related osteonecrosis of the jaws in rats, Photodiagn. Photodyn. Ther. 40 (2022) 103172.

[21] D.W. Williams, K. Ho, A. Lenon, S. Kim, T. Kim, Y. Gwack, R.H. Kim, Long-term ligature-induced periodontitis exacerbates development of bisphosphonate-related osteonecrosis of the jaw in mice, J. Bone Miner. Res. 37 (7) (2022) 1400–1410.

[22] T. Kim, S. Kim, M. Song, C. Lee, H. Yagita, D.W. Williams, E.C. Sung, C. Hong, K. H. Shin, M.K. Kang, N.H. Park, R.H. Kim, Removal of pre-existing periodontal inflammatory condition before tooth extraction ameliorates medication-related osteonecrosis of the jaw-like lesion in mice, Am. J. Pathol. 188 (10) (2018) 2318–2327.

[23] H. Hadad, H.R. Matheus, S.I. Pai, F.A. Souza, F.P.S. Guastaldi, Rodents as an animal model for studying tooth extraction-related medication-related osteonecrosis of the jaw: assessment of outcomes, Arch. Oral Biol. 159 (2024) 105875.

[24] K. Ogata, W. Katagiri, M. Osugi, T. Kawai, Y. Sugimura, H. Hibi, S. Nakamura, M. Ueda, Evaluation of the therapeutic effects of conditioned media from mesenchymal stem cells in a rat bisphosphonate-related osteonecrosis of the jaw-like model, Bone 74 (2015) 95–105.

[25] S. Wu, F. Li, J. Tan, X. Ye, Y. Le, N. Liu, V. Everts, Q. Wan, Porphyromonas gingivalis induces bisphosphonate-related osteonecrosis of the femur in mice, Front. Cell. Infect. Microbiol. 12 (2022) 886411.

[26] R. Yan, R. Jiang, L. Hu, Y. Deng, J. Wen, X. Jiang, Establishment and assessment of rodent models of medication-related osteonecrosis of the jaw (MRONJ), Int. J. Oral Sci. 14 (1) (2022) 41.

[27] A. Soundia, D. Hadaya, Y. Chau, I. Gkouveris, O. Bezouglaia, S. Dry, F. Pirih, T. Aghaloo, S. Tetradis, Local RANKL delivery improves socket healing in bisphosphonate treated rats, Bone 148 (2021) 115945.

[28] R.S. de Molon, S. Cheong, O. Bezouglaia, S.M. Dry, F. Pirih, J.A. Cirelli, T. L. Aghaloo, S. Tetradis, Spontaneous osteonecrosis of the jaws in the maxilla of mice on antiresorptive treatment: a novel ONJ mouse model, Bone 68 (2014) 11–19.

[29] S. Park, K. Kanayama, K. Kaur, H.C. Tseng, S. Banankhah, D.T. Quje, J.W. Sayre, A. Jewett, I. Nishimura, Osteonecrosis of the jaw developed in mice: disease variants regulated by γδ T cells in oral mucosal barrier immunity, J. Biol. Chem. 290 (28) (2015) 17349–17366.

[30] S. Matsuda, T. Fujita, M. Kajiya, K. Takeda, H. Shiba, H. Kawaguchi, H. Kurihara, Brain-derived neurotrophic factor induces migration of endothelial cells through a TrkB-ERK-integrin αVβ3-FAK cascade, J. Cell. Physiol. 227 (5) (2012) 2123–2129.

[31] C. Liao, S. Liang, Y. Wang, T. Zhong, X. Liu, Sclerostin is a promising therapeutic target for oral inflammation and regenerative dentistry, J. Transl. Med. 20 (1) (2022) 221.

[32] C.C. Biguetti, A.H. De Oliva, K. Healy, R.H. Mahmoud, I.D.C. Custódio, D. H. Constantino, E. Ervolino, M.A.H. Duarte, W.D. Fakhouri, M.A. Matsumoto, Medication-related osteonecrosis of the jaws after tooth extraction in senescent female mice treated with zoledronic acid: microtomographic, histological and immunohistochemical characterization, PLoS One 14 (6) (2019) e0214173.

[33] G.I. Brierly, J. Ren, J. Baldwin, S. Saifzadeh, C. Theodoropoulos, M.V. Tsurkan, A. Lynham, E. Hsu, D. Nikolarakos, C. Werner, M.A. Woodruff, D.W. Hutmacher, L. J. Bray, Investigation of sustained BMP delivery in the prevention of medication-related osteonecrosis of the jaw (MRONJ) in a rat model, Macromol. Biosci. 19 (11) (2019) e1900226.

[34] L. Schubert, G. Russmueller, H. Lagler, S. Tobudic, E. Heindel, M. Kundi, C. Steininger, Bone turnover markers can predict healing time in medication-related osteonecrosis of the jaw, Support Care Cancer 29 (12) (2021) 7895–7902.

[35] R. Vlashi, X. Zhang, M. Wu, G. Chen, Wnt signaling: essential roles in osteoblast differentiation, bone metabolism and therapeutic implications for bone and skeletal disorders, Genes Dis 10 (4) (2023) 1291–1317.

[36] Y. Sun, K. Kaur, K. Kanayama, K. Morinaga, S. Park, A. Hokugo, A. Kozlowska, W. H. McBride, J. Li, A. Jewett, I. Nishimura, Plasticity of myeloid cells during oral barrier wound healing and the development of bisphosphonate-related osteonecrosis of the jaw, J. Biol. Chem. 291 (39) (2016) 20602–20616.

[37] H. Mawardi, G. Giro, M. Kajiya, K. Ohta, S. Almazrooa, E. Alshwaimi, S.B. Woo, I. Nishimura, T. Kawai, A role of oral bacteria in bisphosphonate-induced osteonecrosis of the jaw, J. Dent. Res. 90 (11) (2011) 1339–1345.

[38] Y. Zheng, X. Dong, S. Chen, Y. He, J. An, M. Liu, L. He, Y. Zhang, Low-level laser therapy prevents medication-related osteonecrosis of the jaw-like lesions via IL-1RA-mediated primary gingival wound healing, BMC Oral Health 23 (1) (2023) 14.

[39] U. Schirmer, S.A. Schneider, T. Khromov, F. Bremmer, B. Schminke, H. Schliephake, K. Liefeith, P. Brockmeyer, Sclerostin alters tumor cell characteristics of Oral squamous cell carcinoma and may be a key player in local bone invasion, Cells 13 (2) (2024).

[40] J. Zou, W. Zhang, X.L. Li, Effects of SOST gene silencing on proliferation, apoptosis, invasion, and migration of human osteosarcoma cells through the Wnt/β-catenin signaling pathway, Calcif. Tissue Int. 100 (6) (2017) 551–564.

[41] H. Wang, S. Zhao, Y. Liu, F. Sun, X. Huang, T. Wu, Sclerostin suppression facilitates uveal melanoma progression through activating Wnt/β-catenin signaling, Front. Oncol. 12 (2022) 898047.